Joint Computational/Cell-Based Approach for Screening Inhibitors of Tau Oligomerization: A Proof-of-Concept Study

Viet Hoang Man^a, Da Lin^b, Xibing He^a, Jie Gao^{b,*} and Junmei Wang^{a,*}

Accepted 10 June 2022 Pre-press 13 July 2022

Abstract.

Background: Tau assembly produces soluble oligomers and insoluble neurofibrillary tangles, which are neurotoxic to the brain and associated with Alzheimer's and Parkinson's diseases. Therefore, preventing tau aggregation is a promising therapy for those neurodegenerative disorders.

Objective: The aim of this study was to develop a joint computational/cell-based oligomerization protocol for screening inhibitors of tau assembly.

Methods: Virtual oligomerization inhibition (VOI) experiment using molecular dynamics simulation was performed to screen potential oligomerization inhibitors of PHF6 hexapeptide. Tau seeding assay, which is directly related to the outcome of therapeutic intervention, was carried out to confirm a ligand's ability in inhibiting tau assembly formation.

Results: Our protocol was tested on two known compounds, EGCG and Blarcamesine. EGCG inhibited both the aggregation of PHF6 peptide in VOI and tau assembly in tau seeding assay, while Blarcamesine was not a good inhibitor at the two tasks. We also pointed out that good binding affinity to tau aggregates is needed, but not sufficient for a ligand to become a good inhibitor of tau oligomerization.

Conclusion: VOI goes beyond traditional computational inhibitor screening of amyloid aggregation by directly examining the inhibitory ability of a ligand to tau oligomerization. Comparing with the traditional biochemical assays, tau seeding activities in cells is a better indicator for the outcome of a therapeutic intervention. Our hybrid protocol has been successfully validated. It can effectively and efficiently identify the inhibitors of amyloid oligomerization/aggregation processes, thus, facilitate the drug development of tau-related neurodegenerative diseases.

Keywords: Aggregation, EGCG, MD simulation, oligomerization, PHF6, tau protein

INTRODUCTION

Tau protein, which presents in six isoforms with the number of residues ranging from 352 to 441, plays many important physiological roles. Tau constitutes more than 80% of neuronal microtubule associated proteins. It binds to and stabilizes microtubule (MT) [1]. The tau MT binding repeats (R1-R4 spanning residues 244–368) are related to many disease-linked modifications [2]. This region recapitulates much of the aggregation property of tau-441 in animal

^aDepartment of Pharmaceutical Sciences and Computational Chemical Genomics Screening Center, School of Pharmacy, University of Pittsburgh, Pittsburgh, PA, USA

^bDepartment of Neuroscience, The Ohio State University Wexner Medical Center, Columbus, OH, USA

^{*}Correspondence to: Jie Gao, Department of Neuroscience, The Ohio State University Wexner Medical Center, Columbus, OH 43210, USA. Tel.: +1 614 293 8915; E-mail: Jie.Gao@osumc.edu.; Junmei Wang, Department of Pharmaceutical Sciences and Computational Chemical Genomics Screening Center, School of Pharmacy, University of Pittsburgh, Pittsburgh, PA 15261, USA. Tel.: +1 412 383 3268; E-mail: junmei.wang@pitt.edu.

models [3]. Tau protein aggregates into neurotoxic formations including insoluble neurofibrillary tangles (NFT) and soluble oligomers [4, 5], which are associated with several neurodegenerative disorders, including Alzheimer's disease (AD) and Parkinson's disease [6–8]. Inhibition of tau aggregation is a possible avenue to prevent the development of tau-related neurodegenerative diseases. Therefore, the development of an effective protocol which can identify "true" inhibitors of tau aggregation is of great interest [9–14].

A typical protocol of inhibitor screening consists of two stages, the computational screening and experimental confirmation. The first stage focuses on prioritizing ligands mostly based on their binding affinities to the employed drug target, while the second stage confirms the prediction through bioassays. In the case of amyloid aggregation, computational screening filters including docking simulations, endpoint (such as MM-PBSA [15-17]) and alchemical free-energy methods, can be used to estimate the binding energy and/or binding free energy between a ligand and a monomer or aggregates (fibrils) of amyloid peptides/proteins. So far, many aggregates of amyloid peptides/proteins have been resolved by Xray crystallography or Cryo-EM [18-22]. However, binding affinity-based virtual screening is rooted in a hypothesis that the higher the binding affinity of a ligand to amyloid targets is, the better ability it has in inhibiting amyloid aggregation. This hypothesis is not valid since a good binding affinity is needed, but not sufficient to guarantee the ligand is a good inhibitor of amyloid aggregation. Moreover, most bioassays only measure a ligand's ability to inhibit the fibrillar formation in steady of the oligomerization process which produces neurotoxic oligomers. Thus, the conventional screening protocol which has been widely applied in drug lead identification for a well-defined binding pocket may not work for the identification of inhibitors of amyloid aggregation. The above rationale may explain the high failure rate in drug development targeting amyloid peptides.

Recently, we developed a virtual oligomerization inhibition (VOI) method which applies extensive molecular dynamics (MD) simulations to identify "true" inhibitors of $A\beta$ oligomerization. This method can serve as a filter in the computational stage [23]. We have applied the VOI method in ranking the known inhibitors of $A\beta$ aggregation and our prediction is well in agreement with the experimental findings [23]. More importantly, the early aggregation kinetics, with or without an inhibitor

can be characterized at atomistic level through VOI experiment.

In this developed ioint work. we computational/cell-based protocol to effectively identify inhibitors of tau oligomerization. For the computational screening stage, VOI was applied to identify inhibitors of oligomerization process. A full-length tau protein, which may have up to 441 residues, is too large to be applied in tau oligomerization simulation. Therefore, we used PHF6, a tau segment which is essential for tau aggregation and amyloid formation in VOI screening [24]. PHF6 is a hexapeptide of tau protein (Residues 306–311 in R3 repeat) with amino acid sequence of VQIVYK. Note it is a common practice to apply a key fragment in MD simulations of amyloid proteins/peptides. For example, we used both $A\beta_{16-22}$ and the full-length Aβ₁₋₄₂ peptides in conducting VOI experiment for AB oligomerization [23]. For the experimental stage, we did not apply tau aggregation bioassay to confirm the inhibition of a ligand to tau assembly since the current experimental technologies are limited in investigating the dynamics of early tau oligomerization. Instead, we examined whether a ligand could inhibit tau seeding activities in a HEK293 tau biosensor cell line developed by Diamond and co-workers [25, 26]. This cell line expresses tau repeated domain (RD) containing the disease-associated P301S mutation fused to either Cyan Fluorescent Protein (CFP) or Yellow Fluorescent Protein (YFP), and cells produce a fluorescence resonance energy transfer (FRET) signal upon aggregation of tau. As prion-like propagation of proteopathic tau seeds drive the progression of neurodegenerative diseases, measuring the effects of tau oligomerization inhibitor on tau seeding activities in cells should serve as a better indicator for the outcome of therapeutic intervention, comparing with traditional biochemical assays. We tested the developed screening protocol on two known small molecules, Epigallocatechin-3gallate (EGCG) and Blarcamesine (Anavex273). EGCG, a polyphenolic flavonoid extracted from green tea, is considered to have neuroprotective and neuro-rescue effects including modulation of cell survival and cell cycle genes [27]. EGCG can inhibit the aggregation of several proteins including transthyretin protein, Islet amyloid polypeptide (IAPP) and AB peptides [28–30]. Particularly, EGCG has been reported to interact with tau and inhibit tau aggregation in biochemical assays [31]. Anavex273, a drug in clinical trials for the treatment of AD and

Parkinson's disease, was suggested to block tau hyperphosphorylation and protect mitochondria [32, 33]. However, there is no report on Anavex273's inhibitory ability on tau aggregation before, thus it severed as a negative control.

MATERIALS AND METHODS

Computational details

MD simulation protocol

To study the oligomerization of tau fragment, PHF6, we first constructed a control system, 8PHF6, by placing 8 PHF6 peptides at the eight vertices of a 25-Å cube. The 8 PHF6 peptides were random chosen from a structure databank of monomeric PHF6. To obtain the monomeric databank, A PHF6 peptide with the sequence of ACE-VQIVYK-NME was generated by using AMBER tools [34]. The two capping residues, acetyl group (ACE) at N-terminus and methyl group (NME), were added to avoid an artificial strong interaction between termini. The peptide was put in the center of a cubic box solvated by 2200 explicit TIP3P water molecules [35]. This monomeric system underwent 5000 steps of minimization, followed by a 100-ns NPT MD simulation. The PHF6 monomer structure databank was constructed by storing 5000 monomeric structures evenly collected from the last 50 ns of the MD trajectory. To consider impact of a ligand on the oligomerization of PHF6 peptides, an 8PHF6+6ligands system was constructed by adding six ligands to the centers of the six faces of the cube to the 8PHF6 system (Fig. 1). This design gave 3:4 of drug-peptide concentration ratio and provided homogeneous systems to model. All 8PHF6 and 8PHF6+6ligands systems were placed at the center of octahedron box solvated by explicit TIP3P water molecules, and Na+ and Cl- ions were added to neutralize the net charge of the simulation systems and to obtain the salt concentration of 0.15 M. The minimum distance between any atom of the peptide and the edges of the water box was at least 10 Å. The peptides were described by Charmm36m force field [36], which is currently the most suitable to simulate amyloid aggregations [37, 38]. The parameters of the ligands were generated by SwissParam, which provides topology and parameters for small organic molecules compatible with the Charmm all atoms force field [39]. The box size and volume were 78 Å and 365310 Å³. The number of water molecules were 11500 for 8PHF6 system and 11392

for 8PHF6+6ligands. The concentrations of peptide and ligand were 36 mM and 27 mM, respectively. For each system, we collected 10 MD trajectories with different initial structures and the sample details were presented as follows.

The GROMACS 2018 package [40] was employed for all simulations. The solvated systems were minimized using the steepest descent method and were equilibrated for 2 ns at constant pressure (P) of 1atm and temperature (T) of 310 K. The pressure and temperature of the simulations were controlled using the Berendsen coupling method [41] with a relaxation time of 0.1 ps and the Bussi-Donadio-Parrinello velocity scaling method [42] with a relaxation time of 1 ps, respectively. The equations of motion were integrated using a leap-frog algorithm [43] with a time step of 2 femtoseconds (fs). A 1.1 microseconds (µs) NPT sampling simulation was subsequently conducted for post-analysis using the same MD protocol in the equilibration phase. For each system, the total MD simulation time is 11 µs. The LINCS algorithm [44] was used to constrain the lengths of all covalent bonds with a relative geometrical tolerance of 10⁻⁴. The van der Waals forces were calculated with a cutoff of 10 Å, and the particle mesh Ewald method [45] was employed to treat the long-range electrostatic interactions. The nonbonded interaction pair list was updated every 5 fs using a cutoff of 10 Å. Periodic boundary conditions were applied to all the simulations.

Data analysis

The structures of the 8 PHF6 peptides sampled by MD simulations were characterized by intermolecular side chain-side chain contacts, intermolecular backbone hydrogen bond (H-bond), solvent accessible surface areas (SASA) and β -content. A side chain-side chain contact is formed if the distance between the centers of mass of two residue side chains is within 6.5 Å. An H-bond is formed if the acceptor-donor distance is within 3.5 Å and the acceptor-donor-H angle is less than 30°. The β -content was calculated by using the STRIDE algorithm [46, 47], and SASA was calculated by using GROMACS tools.

The aggregation rate of PHF6 peptides was estimated by the formation time of β -sheets and oligomers. The size of β -sheets ranges from 2 to 8 strands, and the oligomers vary from dimer to octamer. The oligomers were classified using the oligomerization contact between peptide pairs. Two peptides are in oligomerization contact if the loss of

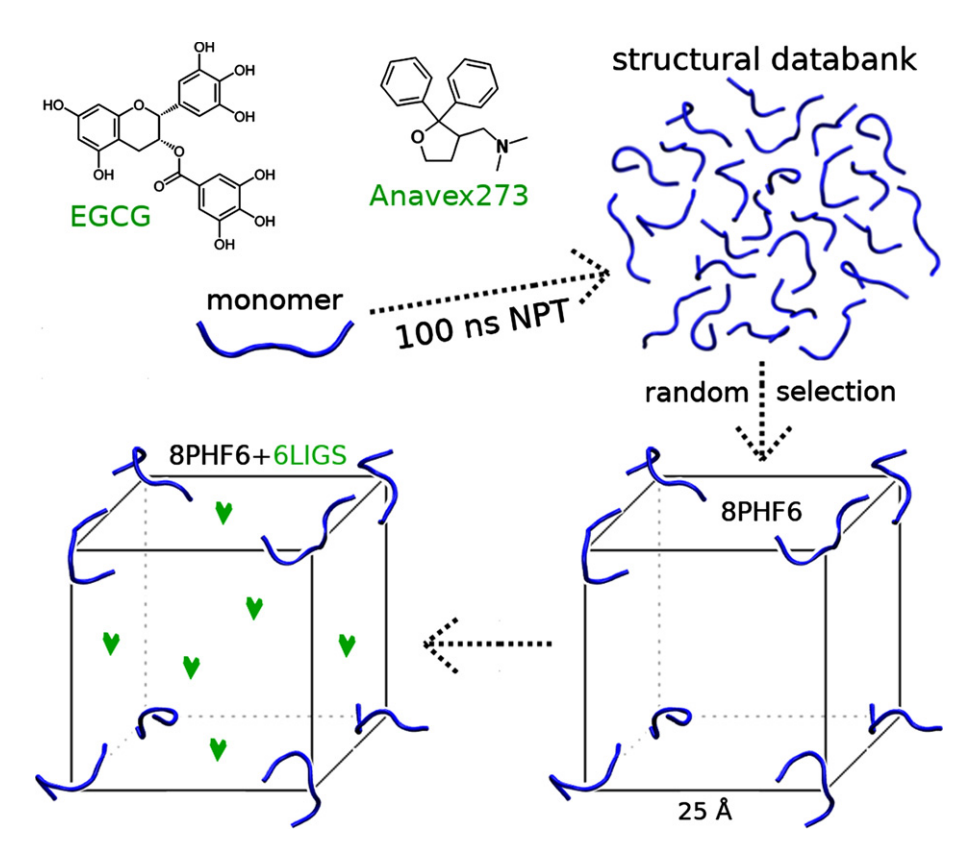


Fig. 1. The 2D structure of EGCG and Anavex273, and the system design. Ligands are presented by green heart. PHF6 peptide is in blue color.

SASA ($SASA_{loss}$), which was calculated by Equation 1, is equal or greater than 10%.

$$SASA_{loss} = 100 \frac{SASA_{P1} + SASA_{P2} - SASA_{P1P2}}{SASA_{P1} + SASA_{P2}}$$
(1)

Here, SASAP1, SASAP2 and SASAP1P2 are SASA of the first peptide (P1), second peptide (P2) and two peptides (P1P2). The oligomerization time $(O\tau)$ of an oligomer is defined as the time period between the beginning of NPT simulation and the timepoint when the oligomer was first formed. The oligomerization inhibition rate (OIR) of a ligand, which measures the inhibitory ability of the ligand, is calculated by Equation 2.

$$OIR = 100 \frac{O\tau_{lig} - O\tau_{control}}{O\tau_{control}}$$
 (2)

Here, $O\tau_{control}$ and $O\tau_{lig}$ are oligomerization time of the PHF6 oligomer in the control and a 8PHF6+6ligands systems, respectively.

Tau seeding assay

Purification of seeding-competent tau fibrils from AD brains

Tau fibril was isolated from a human AD brain as previously described [48]. Human brain tissues from sporadic AD patients, and normal control were obtained from Neurodegenerative Disease Brain Tissue Repository (Buckeye Brain Bank). All cases used were histologically confirmed. For each purification, 5 g of frontal cortical gray matter was homogenized using Dounce homogenizer in 4.5 ml high-salt buffer (10 mM Tris-HCl, pH 7.4, 0.8 M NaCl, 1 mM EDTA, and 2 mM DTT, protease inhibitors) containing 0.1% sarkosyl and 10% sucrose. The lysates were centrifuged at 10,000 g for 10 min at 4 °C, followed by re-extraction once using the same high-salt buffer. Additional sarkosyl was added to the pooled supernatant to reach 1%, and incubated at room temperature for 1 h. Samples were then centrifuged at 300,000 g for 60 min at 4 °C. The resulting sarkosylinsoluble pellets were further purified by a brief sonication using a hand-held probe (QSonica) followed by centrifugation at $100,000 \,\mathrm{g}$ for $30 \,\mathrm{min}$ at $4\,^{\circ}\mathrm{C}$. The pellets were resuspended in PBS, sonicated with 20 short pulses ($\sim 0.5 \,\mathrm{s/pulse}$), and spun at $10,000 \,\mathrm{g}$ for $30 \,\mathrm{min}$ at $4\,^{\circ}\mathrm{C}$ to remove large debris. The final supernatants, which contained enriched pathological tau fibrils, were used in the study, and referred to as AD-tau.

FRET-based tau seeding assay

Tau RD P301S FRET Biosensor cell line (CRL3275) was purchased from ATCC. Tau Biosensor cells were plated at density of 60,000 cells per well in 48-well plates. Cells are 50-60% confluent 24 h after plating. AD-tau was transduced into cells using Lipofectamine. Transduction complexes were made by mixing Lipofectamine 2000 (Invitrogen) with AD tau in Opti-MEM and incubated in room temperature for 30 min before adding to cells. Chemicals at various concentration were added to cells 2 h after transduction of AD tau seeds. 24 h later, cells were fixed with 4% paraformaldehyde and nucleus were stained with DAPI. To measure FRET, cells were excited at 405 nm, and fluorescence was captured with 525/50 nm filters. To quantify FRET, we measured FRET positive area and then normalized it to DAPI area.

RESULTS

VOI experiment using PHF6 peptide

To study the oligomerization of tau PHF6 fragment with and without the presence of a ligand using MD simulation, we considered 8PHF6 and 8PHF6+6ligands simulation systems (Fig. 1). To draw an overall picture of the inhibitory effect of a ligand on PHF6 aggregation, we calculated time dependence of four overall structural parameters of PHF6 peptides including SASA, β-content, number of intermolecular side chain-side chain contacts (N_{SC}), and number of intermolecular main-chain hydrogen bonds (N_{HB}) in the different systems. As shown in Fig. 2, EGCG demonstrated strongly inhibitory effect on the aggregation of PHF6 peptides, while Anavex273 did very little. For all systems, all the parameters charactering PHF6 oligomerization dramatically changed in the first 300 nanoseconds (ns) of the simulation time, but much less fluctuated in the last 800 ns. The population distribution of the radius of gyration (R_g), SASA, N_{SC} and N_{HB} of eight PHF6 peptides from the last 800 ns of the simulations for different systems were shown in

Supplementary Figure 1. The locations of the highest peaks followed the same trend for the R_a and SASA populations, which was opposite to that for the N_{SC} and N_{HB} populations. For the control and 8PHF6+6Anavex273 system, the highest peaks of R_q and SASA populations were located at smaller values of the parameters compared to the 8PHF6+6EGCG system. To make a quantitative comparison, we calculated the averages of the parameters over the last 800 ns of MD simulation time. For SASA, the average values are 52, 53, and 60 nm² for the 8PHF6, 8PHF6+6Anavex273 and 8PHF6+6EGCG systems, respectively; for β-content, the average values are 25%, 27%, and 15% for the three corresponding systems; for N_S, the averages are 43, 40, and 29 for the three corresponding systems; and for N_{HB}, the corresponding values are 13, 13, and 7. Apparently, the values for 8PHF6+6EGCG were significantly different from the corresponding ones for the 8PHF6 and 8PHF6+6Anavex273 systems. These data suggested that EGCG can inhibit β-sheet formation and the interaction between PHF6 peptides, while Anavex273 cannot. This conclusion is also supported by the intermolecular side-side interaction maps of PHF6 peptides in the three systems (Supplementary Figure 2).

During the procedure of PHF6 aggregation, monomers gather and undergo conformational changes resulting in the formation of PHF6 oligomers and β-sheet structures. The size of oligomers and β-sheets increases during the aggregation process. We further evaluated the impact of a ligand on the formations of PHF6 oligomers and β-sheets. Figure 3 illustrated the population distributions of different PHF6 \(\beta\)-sheets (Fig. 3a) and oligomers (Fig. 3b). Similar to the time course of the overall structural parameters, the population distributions of the β-sheets and oligomers for the control system were quite similar to those for 8PHF6+6Anavex273, but distinct to those for 8PHF6+6EGCG. For 8PHF6+6Anavex273 system, the populations of large oligomers (pentamer, hexamer, and heptamer), particularly 5BS, were higher than those in the control system, indicating that Anavex273 slightly enhances the aggregation of PHF6 peptides. For the 8PHF6+6EGCG system, the populations of all β -sheet sheets ($n\beta S$, n ranges from 2 to 8) were smaller than the corresponding ones for the control system. This result again implied that EGCG inhibited the β-sheet formation during the PHF6 oligomerization process. As long as the oligomeric formation is concerned, the population distributions

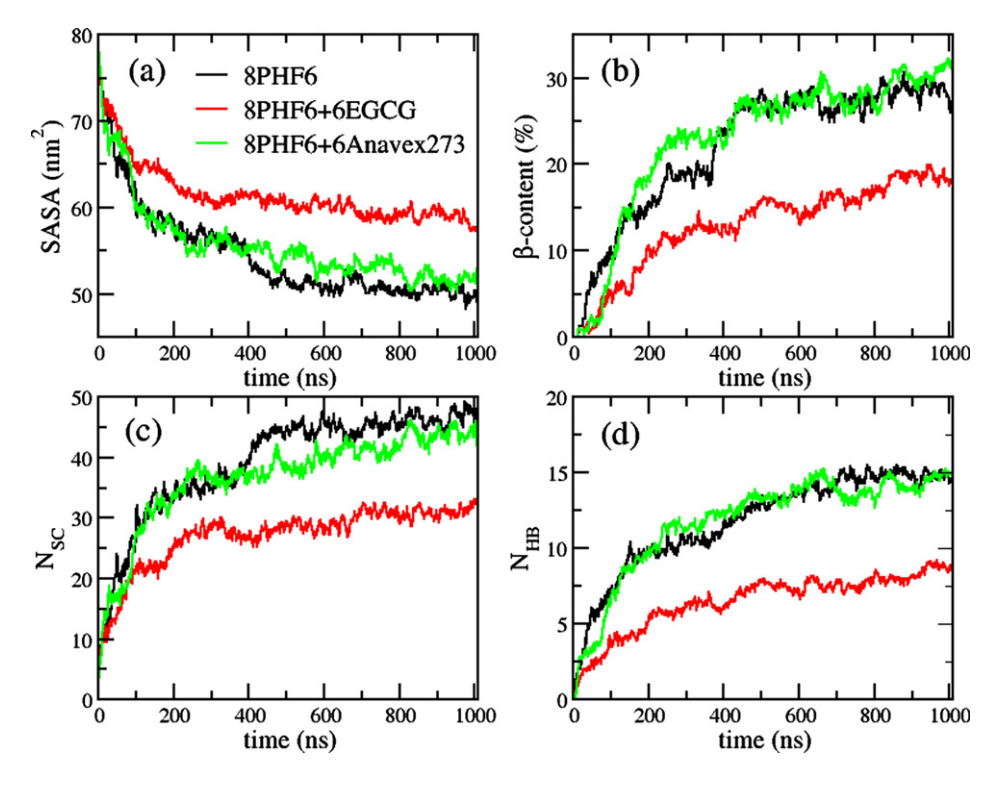


Fig. 2. Evolution of SASA (a), β -content (b), number of side chain-side chain contacts (c), and number of main-chain hydrogen bonds (d) of PHF6 peptides in different systems, 8PHF6 (Control), 8PHF6+6EGCG (+EGCG) and 8PHF6+6Anavex273 (+Anavex273). The data were averaged from 10 trajectories for each system.

are size-dependent. For small-sized oligomers like dimer, trimer and tetramer, the 8PHF6+6EGCG system had larger population sizes than the control system and 8PHF6+6Anavex273, while for the large-sized oligomers like pentamer, hexamer, heptamer and octamer, the trend is just the opposite. This result suggests that EGCG can effectively inhibit the growth of PHF6 oligomers. Moreover, this conclusion is also supported by the PHF6 oligomerization time $(O\tau)$ of the three systems, and the PHF6 oligomerization inhibition rate (OIR) of the two ligand-containing systems (Table 1).

Amyloid aggregates, soluble oligomers, and insoluble fibrils are toxic to the brain and can lead to brain damage [49]. For the case of tau proteins and $A\beta$ peptides, recent evidence showed that oligomers are more toxic than fibrils [4, 5, 50, 51]. Furthermore, it was found that smaller $A\beta$ oligomers are usually more toxic than larger oligomers, and the toxic size of $A\beta$ oligomers maybe as small as a dimer [52–56]. Interestingly, previous studies also pointed out that tetramer is more toxic than dimer and trimer [53, 55, 57, 58]. Those results suggest that tetramer may be the most toxic $A\beta$ oligomer [53, 57]. Assuming that

PHF6 peptide is similar to Aβ peptide in term of the size and formation toxic dependence of the aggregates, Anavex273 may reduce the toxicity of PHF6 oligomerization by accelerating the transformation from oligomers to fibrils. In contrast, Fig. 3b showed the populations of small PHF6 oligomers including dimer, trimer, and tetramer in 8PHG6+6EGCG system were significantly higher than those in the ligand-free 8PHF6 system. It indicates that EGCG could enhances the formation of the small oligomers. Can we, hereby, conclude that EGCG may be not really a good inhibitor? Not really, as the data in Fig. 3 was from the last 800 ns of the 1000 ns simulation, and it did not include the rapidly changing process of the oligomerization in the first 200 ns. Additionally, the data of the oligomerization time and oligomerization inhibition rate (Table 1) showed that EGCG slowed down the formation of the small oligomers to some degree. Thus, to depict the complete picture of how EGCG interfering with the formation of the small oligomers, we need to also consider the population change of the small oligomers during the first 200 ns. As shown in Supplementary Figure 3, EGCG did enhance the dimeric formation, and had

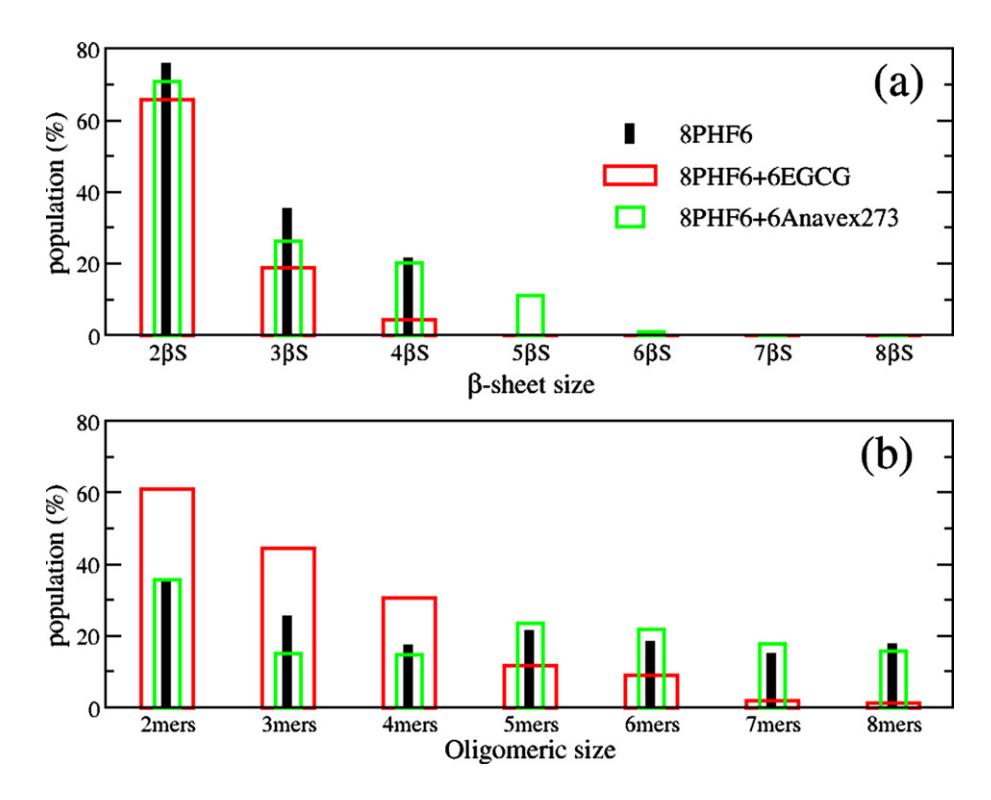


Fig. 3. The population of nβS (a) and oligomers (b) of PHF6 peptides in different systems, 8PHF6 (Control), 8PHF6+6EGCG (+EGCG) and 8PHF6+6Anavex273 (+Anavex273). The data were calculated from 10 trajectories for each system and the last 800 ns of each trajectory.

Table 1 Oligomerization time (O τ) of PHF6 oligomers, and oligomerization inhibition rate (OIR) of the ligands. The averaged OIR was calculated from the OIRs of trimer, tetramer, ..., and octamer. Because dimers were fast formed in all system (O τ < 3 ns), dimeric OIR was not considered

System	PAR	Dimer	Trimer	Tetramer	Pentamer	Hexamer	Heptamer	Octamer	Average
8PHF6	Oτ (ns)	<3	5	15	25	51	72	170	
8PHF6	$O\tau$ (ns)	<3	7	17	49	77	157	381	
+6EGCG	OIR (%)	NA	40	13	96	51	118	124	74
8PHF6	$O\tau$ (ns)	<3	7	17	22	50	70	179	
+6Anavex273	OIR (%)	NA	40	13	-12	-2	-3	5	7

little effect on the trimeric formation, but significantly slowed down/inhibited the formation of tetramers in the first 200 ns of simulations. Considering tetramer may be the most toxic oligomer of the tau hexapeptide fragment (like $A\beta$ peptide), the data of overall structures (Fig. 2 and Supplementary Figure 1) as well as intermolecular side chain-side chain interaction map (Supplementary Figure 2), support the conclusion that EGCG is a good inhibitor of tau oligomerization.

As EGCG demonstrated a strong inhibitory effect against PHF6 oligomer formation, we further investigated the interactions between heavy atoms of EGCG and PHF6 residues (Fig. 4). An EGCG atom and a PHF6 residue is in the interaction state when their

distances are equal to or smaller than 0.3 nm. Among six residues of PHF6, Y310 had the highest frequency interacting with EGCG, followed by I308, Q307, and V309. Interestingly, K311, although has similar size as Y310 and I308, interacted with EGCG much less frequently. This observation indicated that EGCG preferred to interact with hydrophobic residues. Among the 33 heavy atoms of EGCG, most oxygen atoms in the hydroxyl or carbonyl functional groups showed strong interactions with PHF6 peptides. This is reasonable because those oxygen atoms appear on the surface of EGCG, thus have higher probability to interact with PHF6 peptides than the other atoms.

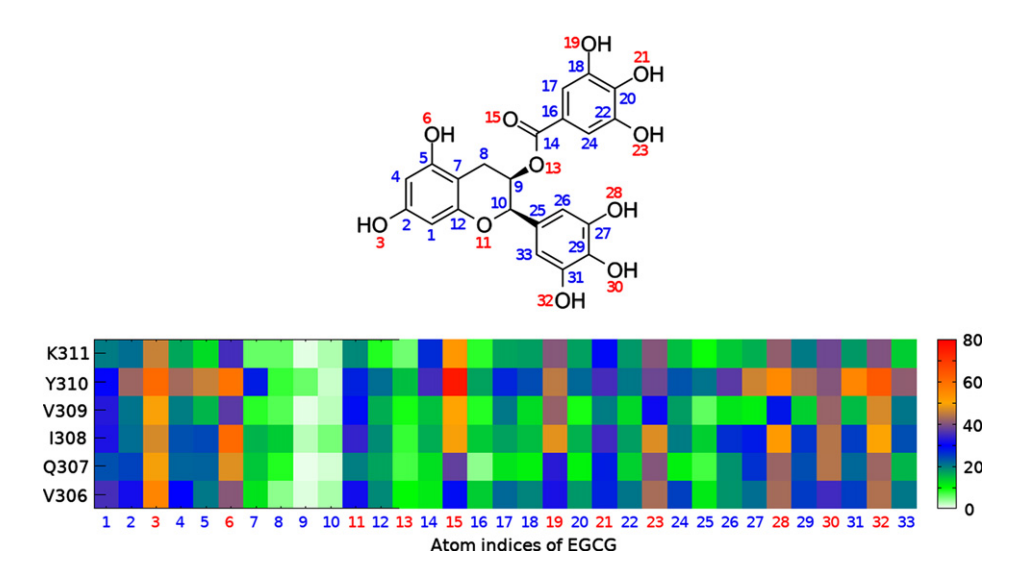


Fig. 4. Interaction map between heavy atoms of EGCG and residues of PHF6 peptide. The color bar indicates population (in %) of the interaction. The index number of oxygen atoms is in red color, while the index of other atoms is blue. The data were calculated from 10 trajectories for each system and the last 800 ns of each trajectory.

FRET-based cell assay to evaluate inhibitors for tau oligomerization

Prion-like propagation of tau aggregates underlie the progression of neurodegenerative diseases, including AD and the related tauopathies. To experimentally validate the inhibitors of tau oligomerization identified in MD simulation, we assessed the ability of EGCG and anavex273 to inhibit tau seeding activities in a HEK293 tau biosensor cell line [59]. Proteopathic tau fibrils used in the seeding assay were directly purified from postmortem AD patient brains, thus better representing the unique conformational features of tau seeds that develop in AD brains. To prepare seeding-competent tau fibrils, we obtained frozen brain tissues from human non-AD or age-matched sporadic AD-patients from Buckeye Brain Bank at The Ohio State University. AD brains used were histologically confirmed to contain NFTs using X34, a highly fluorescent marker for β-sheet structures (Fig. 5A). Pathological tau fibrils were extracted from sarkosyl-insoluble fractions by ultracentrifugation as described previously [48]. Repeated washing and centrifugation of sarkosylinsoluble fraction (P1-3) yielded enriched tau protein (HT7) (Fig. 5B) with pathological phosphorylation at Ser202/Thr205 (AT8) (Fig. 5C). Final P3 fraction is used as tau seeds (AD-tau) for our FRET-based cell assay.

In tau FRET Biosensor cell, AD-tau convert tau RD into the aggregated states displaying as punctate and

reticular intracellular inclusions in a dose-dependent manner (Fig. 6A, B), suggesting AD-tau is seed-competent. Then we tested the ability of anavex273 and EGCG to inhibit tau seeding activities. Chemicals at various concentrations were added into biosensor cells 2 h after AD-tau seeds transduction. Anavex273 did not inhibit tau seeding at all the concentrations tested (up to $20 \,\mu g/ml$). Conversely, EGCG strongly inhibits tau seeding with IC50 estimated at 1.25 $\,\mu g/ml$ (Fig. 6C, D). This data is consistent with our MD simulation results that only EGCG strongly inhibits the aggregation of PHF6 peptides.

DISCUSSION

The aggregation of tau protein leads to the accumulation of NFTs, which is one of the two major pathological hallmarks in the brain of an AD patient [60]. Mounting evidence now suggests tau aggregates (or seeds) nucleate the fibrillization of endogenous tau monomer upon internalization into cell, thus transmitting the aggregated state from cell-to-cell via prion-like mechanisms. Screening compounds which can inhibit tau aggregation, particularly oligomerization, is of great interest to develop novel therapeutic agents for AD. Numerous studies have been conducted to identify inhibitors of tau assembly, and to investigate the inhibition mechanisms [9, 10, 12, 13, 31, 61–67]. Most of the studies only applied experimental approaches to examine tau aggrega-

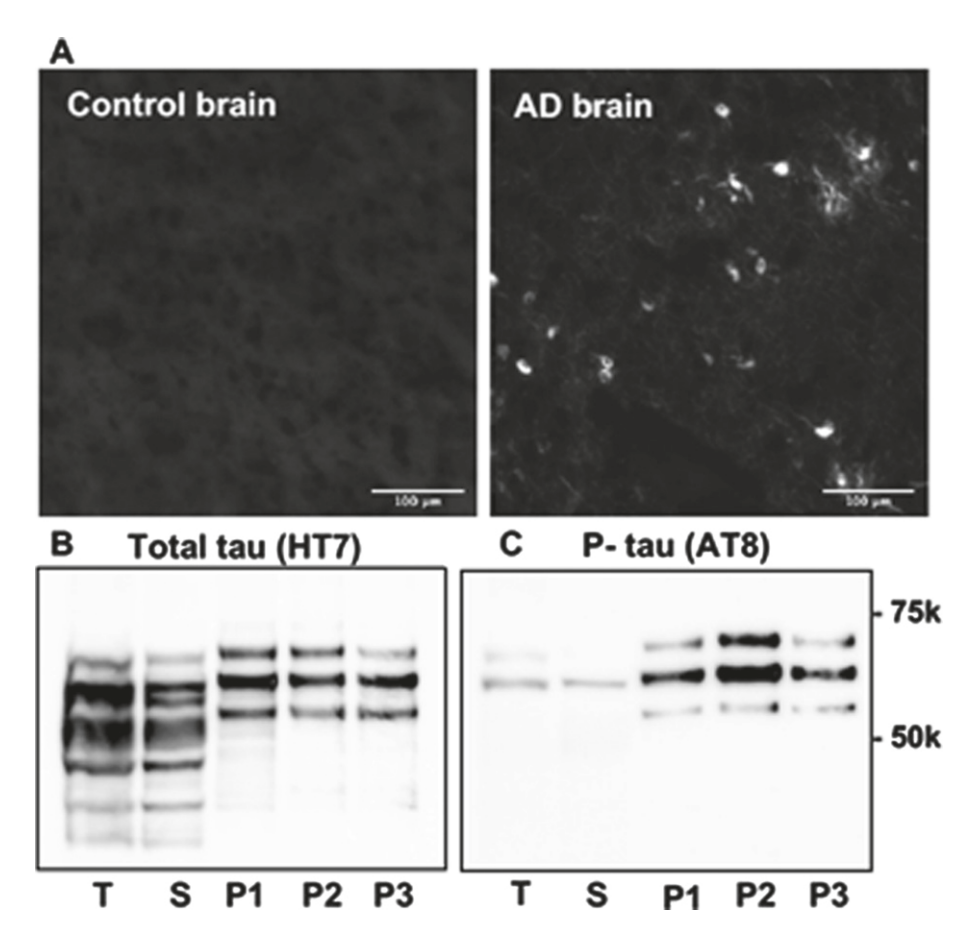


Fig. 5. Preparation of tau fibrils from AD patient brains. A) Representative neurofibrillary tangles X34-staining in postmortem AD brains and age-matched controls. Different fractions from tau fibrils purification were immunoblotted with HT7 (a pan-Tau antibody) (B) and AT8 (C) (a monoclonal antibody specific phospho-Tau at Ser202 and Thr205). T: total lysates, S, supernatant; P1-P3, Sarkosyl-insoluble pellets.

tion, and to estimate binding affinity of a ligand to tau protein/aggregates [9, 10, 12, 13, 31, 61-67]. The experiments applied in the previous studies can only identify the binding affinity of a ligand to tau protein and/or the inhibition of the ligand to tau aggregation into fibrils/protofibrils. However, because of current technology limitations, they did not determine whether the ligand inhibits the early tau oligomerization directly. For example, ThT fluorescence and EM assays are only able to identify the inhibition of a ligand to tau fibrillar formation, but not to tau oligomerization. SDS-PAGE analysis is usually used to characterize oligomers, the effect of sodium dodecyl sulfate on the oligomerization can lead to flawed information [68]. Additionally, the early amyloid oligomerization process happens very fast as the monomeric concentrations used in vitro studies, ranging from micromolar to denser range, are dramatically higher than the monomeric

concentration in physiological condition. Thus, the picture of oligomerization inhibition is too difficult to be accurately described. Although computational approaches can complement experimental means by providing ligand protein interactions at atomistic level, the computational methods employed in the previous studies only examined the binding affinity and interaction of an inhibitor to tau aggregates (protofibril/fibrils) [31, 66]. The inhibition activities of an inhibitor on early tau oligomerization have not been studied yet.

The computational methods applied in a traditional inhibitor screening for a protein aggregation mostly focus on binding affinity of a ligand to protein aggregates. Those approaches assume that the stronger binding to the protein aggregates a ligand has, the better inhibition to the aggregation the ligand can. Despite this hypothesis have been validated in some studies of A β aggregates [69–71], it may be incorrect

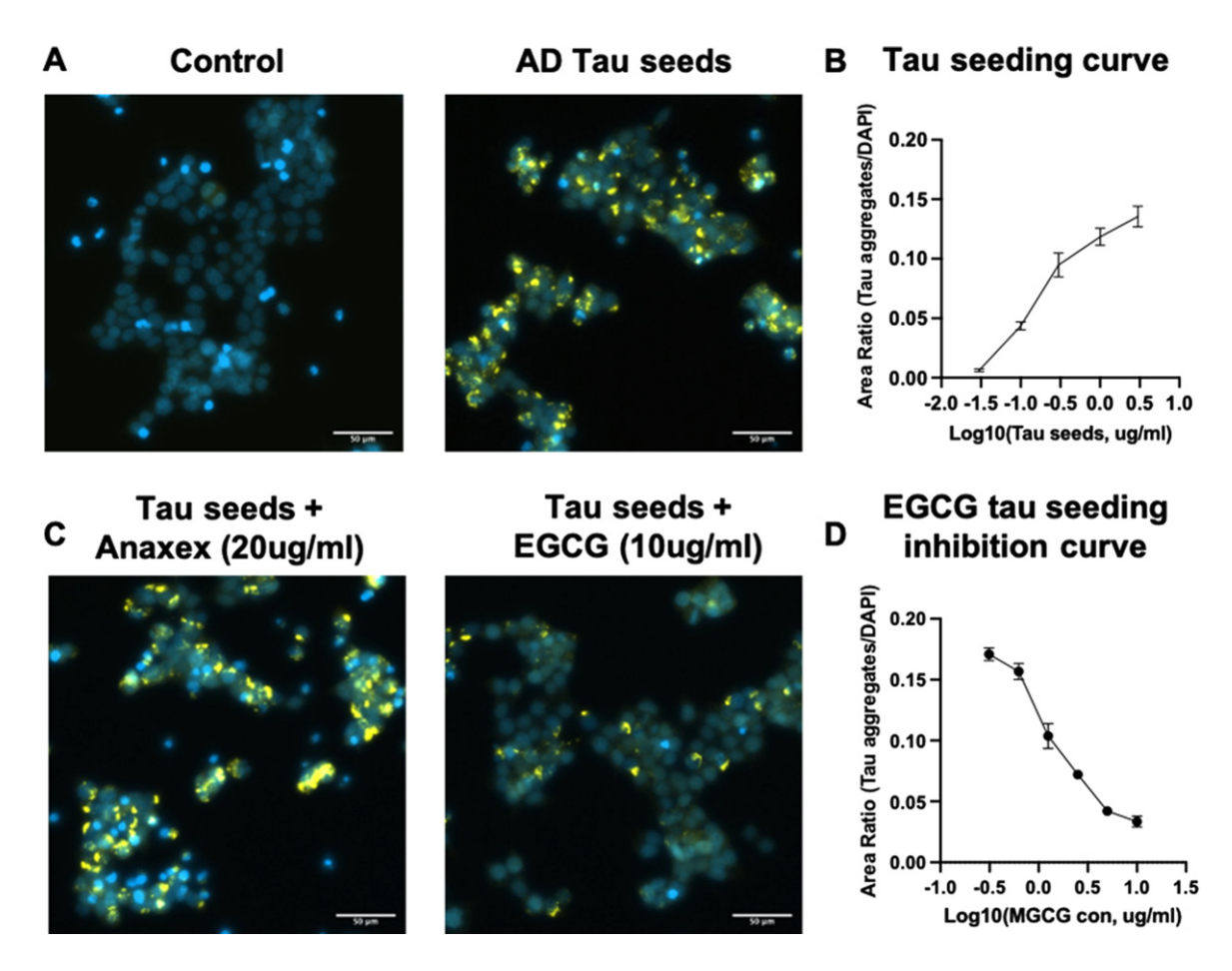


Fig. 6. EGCG inhibits AD-tau seeding in the tau biosensor cell line. A) Representative images of tau biosensor cells transduced with liposome vehicles or tau seeds ($5 \mu g/ml$). tau treated cells exhibit intracellular tau inclusions. (Scale bar, $50 \mu M$). B) AD-tau seeds promote tau aggregation in a dose-dependent manner. C) Representative images of tau biosensor cells transduced with tau seeds ($5 \mu g/ml$) and treated with Anavex273 ($20 \mu g/ml$) or EGCG ($10 \mu g/ml$). (Scale bar, $50 \mu M$). D) EGCG inhibits tau seeding in a dose-dependent manner.

for the dynamic process of amyloid oligomerization. To re-examine this hypothesis, we first performed docking screening for a compound library. The library contains 702 small molecules which have 85% of similarity to at least one of known amyloid aggregation inhibitors including EGCG, brazilin and curcumin. The docking targets are six tau aggregates deposited in PDB databank (Supplementary Figure 4). Based on the docking result, we selected two compounds, ZINC00668105 and ZINC78502846, which showed high binding affinities to the tau aggregates, to advance to the VOI experiment using PHF6 peptide. The binding affinities of Anavex273, EGCG, ZINC00668105, and ZINC78502846 to the six tau aggregates are shown in Supplementary Table 1. The impact of ZINC00668105 and ZINC78502846 on the oligomerization of PHF6 peptides were shown on Supplementary Figures 5 and 6 and summarized in

Supplementary Table 2. It is shown that the binding affinities of the ligands to the tau aggregates were in the order of ZINC00668105 \sim ZINC78502846 (-8.5 kcal/mol)>EGCG (-7.7 kcal/mol)>Anavex273 (-5.6 kcal/mol), while the inhibition abilities of the ligands to the PHF6 oligomerization were in the order of EGCG>ZINC00668105>ZINC 78502846 > Anavex273. This result indicated that a weaker binder of tau aggregates, such as Anavex2763, is unlikely to become a strong inhibitor of PHF6 oligomerization; On the other hand, a strong binder of tau aggregates, such as ZINC78502846, may not be necessary a good inhibitor of PHF6 oligomerization. Encouragingly, the results of VOI and tau seeding assay are totally consistent, i.e., the better a ligand can interfere with PHF6 oligomerization, the stronger inhibition affinity it has in the tau seeding assay. Thus, our hybrid protocol of applying VOI simulation and tau seeding assay represents a promising approach to identify inhibitors of tau oligomerization.

We have shown that VOI could improve the accuracy in screening inhibitors for amyloid oligomerization. However, it is also much more computer time and resource demanding than the traditional computational methods of binding affinity estimation such as docking simulation, end-point MM-PBSA [15, 16] and pathway-based free-energy perturbation (FEP) [72]. For example, to examine a compound using an Intel (R) CPU. E5-2690 (2.6 GHz), it will take around 97000 CPU hours for VOI, 5 CPU hours for docking and 3000 CPU hours for MM-PBSA and FEP. Therefore, this limitation of VOI should be bear in mind, and we recommend using VOI as an extra filter to further prioritize the top leads from the binding affinity estimations in a traditional inhibitor screening of amyloid oligomerization.

Conclusion

In this proof-of-concept study, we have introduced and evaluated a screening protocol which consists of VOI simulation and tau seeding assay. VOI goes beyond traditional computational inhibitor screening of amyloid aggregation by directly examining the inhibitory ability of a ligand to tau oligomerization through large-scale MD simulations. Taking the advantage of the novel computational method, we were able to directly track the dynamics of tau fragment oligomerization with and without the presence of ligands as well as reveal the interactions between ligand and tau peptides at atomic level. In addition, comparing with the traditional biochemical assays, tau seeding activities in cells is a better indicator for the outcome of a therapeutic intervention. This hybrid protocol has been successfully validated using EGCG and Anavex273. Both in silico and in vitro methods suggested that EGCG can inhibit tau aggregation and seeding while Anavex273 cannot. In a conclusion, our hybrid screening protocol is able to effectively and efficiently identify the inhibitors of amyloid oligomerization/aggregation processes, thus, can be beneficial to the drug development of tau-related neurodegenerative diseases.

ACKNOWLEDGMENTS

This work was supported by the funds from the National Institutes of Health (NIH) NIH R01GM079383, NIH K25AG070277, the National Science Foundation (NSF) NSF1955260, and The Chronic Brain Injury (CBI) Pilot Award at The Ohio State University. The authors also thank the computing resources provided by the Center for Research Computing (CRC) at University of Pittsburgh.

Authors' disclosures available online (https://www.j-alz.com/manuscript-disclosures/22-0450r1).

SUPPLEMENTARY MATERIAL

The supplementary material is available in the electronic version of this article: https://dx.doi.org/10.3233/JAD-220450.

REFERENCES

- Kadavath H, Hofele RV, Biernat J, Kumar S, Tepper K, Urlaub H, Mandelkow E, Zweckstetter M (2015) Tau stabilizes microtubules by binding at the interface between tubulin heterodimers. *Proc Natl Acad Sci U S A* 112, 7501-7506.
- [2] Spillantini MG, Goedert M (2013) Tau pathology and neurodegeneration. *Lancet Neurol* 12, 609-622.
- [3] Stöhr J, Wu H, Nick M, Wu Y, Bhate M, Condello C, Johnson N, Rodgers J, Lemmin T, Acharya S, Becker J, Robinson K, Kelly MJS, Gai F, Stubbs G, Prusiner SB, DeGrado WF (2017) A 31-residue peptide induces aggregation of tau's microtubule-binding region in cells. Nat Chem 9, 874-881.
- [4] Shafiei SS, Guerrero-Munoz MJ, Castillo-Carranza DL (2017) Tau oligomers: Cytotoxicity, propagation, and mitochondrial damage. Front Aging Neurosci 9, 83.
- [5] Cline EN, Bicca MA, Viola LV, Klein WL (2018) The amyloid-oligomer hypothesis: Beginning of the third decade. *J Alzheimers Dis* 64, S567-S610.
- [6] Polymeropoulos MH, Lavedan C, Leroy E, Ide SE, Dehejia A, Dutra A, Pike B, Root H, Rubenstein J, Boyer R, Stenroos ES, Chandrasekharappa S, Athanassiadou A, Papapetropoulos T, Johnson WG, Lazzarini AM, Duvoisin RC, Iorio GD, Golbe LI, Nussbaum RL (1997) Mutation in the α-synuclein gene identified in families with Parkinson's disease. *Science* 276, 2045-2047.
- [7] Hardy J, Selkoe DJ (2002) The amyloid hypothesis of Alzheimer's disease: Progress and problems on the road to therapeutics. *Science* 297, 353-356.
- [8] Singleton AB, Farrer M, Johnson J, Singleton A, Hague S, Kachergus J, Hulihan M, Peuralinna T, Dutra A, Nussbaum R, Lincoln S, Crawley A, Hanson M, Maraganore D, Adler C, Cookson MR, Muenter M, Baptista M, Miller D, Blancato J, Hardy J, Gwinn-Hardy K (2003) α-Synuclein locus triplication causes Parkinson's disease. Science 302, 841.
- [9] Bulic B, Pickhardt M, Khlistunova I, Biernat J, Mandelkow EM, Mandelkow E, Waldmann H (2007) Rhodanine-based Tau aggregation inhibitors in cell models of tauopathy. *Angew Chem Int Ed* 46, 9215-9219.
- [10] Larbig G, Pickhardt M, Lloyd DG, Schmidt B, Mandelkow E (2007) Screening for inhibitors of Tau protein aggregation into Alzheimer paired helical filaments: A ligand based approach results in successful scaffold hopping. Curr Alzheimer Res 4, 1567-2050.

- [11] Bulic B, Pickhardt M, Schmidt B, Mandelkow EM, Waldmann H, Mandelkow E (2009) Development of tau aggregation inhibitors for Alzheimer's disease. *Angew Chem Int Ed* 48, 1740-1752.
- [12] Crowe A, Huang W, Ballatore C, Johnson RL, Hogan AL, Huang R, Wichterman J, McCoy J, Huryn D, Auld DS, Smith AB, Inglese J, Trojanowski JQ, Austin CP, Brunden KR, Lee VM (2009) Identification of aminoth-ienopyridazine inhibitors of Tau assembly by quantitative high-throughput screening. *Biochem* 48, 7732-7745.
- [13] Crowe A, Ballatore C, Hyde E, Trojanowski JQ, Lee VM (2007) High throughput screening for small molecule inhibitors of heparin-induced tau fibril formation. *Biochem Biophys Res Commun* 358, 1-6.
- [14] Malafaia D, Albuquerque HM, Silva AM (2021) Amyloidβ and tau aggregation dualinhibitors: A synthetic and structure-activity relationship focused review. Eur J Med Chem 214, 113209.
- [15] Kollman PA, Massova I, Reyes C, Kuhn B, Huo S, Chong L, Lee M, Lee T, Duan Y, Wang W, Donini O, Cieplak P, Srinivasan J, Case DA, Cheatham TE 3rd (2000) Calculating structures and free energies of complex molecules: Combining molecular mechanics and continuum models. Acc Chem Res 33, 889-897.
- [16] Wang J, Morin P, Wang W, Kollman PA (2001) Use of MM-PBSA in reproducing the binding free energies to HIV-1 RT of TIBO derivatives and predicting the binding mode to HIV-1 RT of efavirenz by docking and MM-PBSA. J Am Chem Soc 123, 5221-5230.
- [17] Wang E, Sun H, Wang J, Wang Z, Liu H, Zhang JZH, Hou T (2019) End-point binding free energy calculation with MM/PBSA and MM/GBSA: Strategies and applications in drug design. *Chem Rev* 119, 9478-9508.
- [18] Wälti MA, Ravotti F, Arai H, Glabe CG, Wall JS, Böckmann A, Güntert P, Meier BH, Riek R (2016) Atomic-resolution structure of a disease-relevant Aβ(1-42) amyloid fibril. Proc Natl Acad Sci U S A 113, E4976-E4984.
- [19] Gremer L, Scholzel D, Schenk C, Reinartz E, Labahn J, Ravelli RBG, Tusche M, Lopez-Iglesias C, Hoyer W, Heise H, Willbold D, Schröder GF (2017) Fibril structure of amyloid-β(1-42) by cryo-electron microscopy. *Science* 358, 116-119.
- [20] Kollmer M, Close W, Funk L, Rasmussen J, Bsoul A, Schierhorn A, Schmidt M, Sigurdson CJ, Jucker M, Fandrich M (2019) Cryo-EM structure and polymorphism of Aβ amyloid fibrils purified from Alzheimer's brain tissue. *Nat Commun* 10, 4760-4760.
- [21] Arakhamia T, Lee CE, Carlomagno Y, Duong DM, Kundinger SR, Wang K, Williams D, DeTure M, Dickson DW, Cook CN, Seyfried NT, Petrucelli L, Fitzpatrick AWP (2020) Posttranslational modifications mediate the structural diversity of tauopathy strains. *Cell* 180, 633-644.
- [22] Zhang W, Tarutani A, Newell KL, Murzin AG, Matsubara T, Falcon B, Vidal R, Garringer HJ, Shi Y, Ikeuchi T, Murayama S, Ghetti B, Hasegawa M, Goedert M, Scheres SHW (2020) Novel tau filament fold in corticobasal degeneration. *Nature* 580, 283-287.
- [23] Man VH, He X, Ji B, Liu S, Xie X, Wang J (2020) Introducing virtual oligomerization inhibition to identify potent inhibitors of Aβ oligomerization. *J Chem Theory Comput* 16, 3920-3935.
- [24] Mohamed N, Herrou T, Plouffe V, Piperno N, Leclerc N (2013) Spreading of tau pathology in Alzheimer's disease by cell-to-cell transmission. *Eur J Neurosci* 37, 1939-1948.

- [25] Mirbaha H, Chen D, Morazova OA, Ruff KM, Sharma AM, Liu X, Goodarzi M, Pappu RV, Colby DW, Mirzaei H, Joachimiak LA, Diamond MI (2018) Inert and seedcompetent tau monomers suggest structural origins of aggregation. Elife 7, e36584.
- [26] Sharma AM, Thomas TL, Woodard DR, Kashmer OM, Diamond MI (2018) Tau monomer encodes strains. *Elife* 7, e37813.
- [27] Levites Y, Amit T, Youdim MBH, Mandel S (2002) Involvement of protein kinase C activation and cell survival/cell cycle genes in green tea polyphenol (-)-epigallocatechin 3-gallate neuroprotective action. *J Biol Chem* 277, 30574-30580.
- [28] Ferreira N, Cardoso I, Domingues MR, Vitorino R, Bastos M, Bai G, Saraiva MJ, Almeida MR (2009) Binding of epigallocatechin-3-gallate to transthyretin modulates its amyloidogenicity. FEBS Lett 583, 3569-3576.
- [29] Meng F, Abedini A, Plesner A, Verchere CB, Raleigh DP (2010) The flavanol (-)epigallocatechin 3-gallate inhibits amyloid formation by islet amyloid polypeptide, disaggregates amyloid fibrils, and protects cultured cells against IAPP-induced toxicity. *Biochemistry* 49, 8127-8133.
- [30] Ehrnhoefer DE, Bieschke J, Boeddrich A, Herbst M, Masino L, Lurz R, Engemann, S, Pastore A, Wanker EE (2008) EGCG redirects amyloidogenic polypeptides into unstructured, off-pathway oligomers. *Nat Struct Mol Biol* 15, 558-566.
- [31] Sonawane SK, Chidambaram H, Boral D, Gorantla NV, Balmik AA, Dangi A, Ramasamy S, Marelli UK, Chinnathambi S (2020) EGCG impedes human tau aggregation and interacts with tau. Sci Rep 10, 12579.
- [32] Lahmy V, Meunier J, Malmstram S, Naert G, Givalois L, Kim SH, Villard V, Vamvakides A, Maurice T (2013) Blockade of tau hyperphosphorylation and Aβ₁₋₄₂ generation by the aminotetrahydrofuran derivative ANAVEX2-73, a mixed muscarinic and σ₁ receptor agonist, in a nontransgenic mouse model of Alzheimer's disease. *Neuropsychopharmacology* 38, 1706-1723.
- [33] Lahmy V, Long R, Morin D, Villard V, Maurice T (2015) Mitochondrial protection by the mixed muscarinic/ÏC1 ligand ANAVEX2-73, a tetrahydrofuran derivative, in Aβ₂₅₋₃₅ peptide-injected mice, a nontransgenic Alzheimer's disease model. Front Cell Neurosci 8, 463.
- [34] Case DA, et al. (2019) "AMBER 19"; University of California: San Francisco.
- [35] Jorgensen WL, Chandrasekhar J, Madura JD, Impey RW, Klein ML (1983) Comparison of simple potential functions for simulating liquid water. J Chem Phys 779, 926-935.
- [36] Huang J, Rauscher S, Nawrocki G, Ran T, Feig M, de Groot BL, Grubmüller H, MacKerell AD Jr (2017) CHARMM36m: An improved force field for folded and intrinsically disordered proteins. *Nat Methods* 14, 71-73.
- [37] Man VH, He X, Derreumaux P, Ji B, Xie X, Nguyen PH, Wang J (2019) Effects of all-atom molecular mechanics force fields on amyloid peptide assembly: The case of Aβ₁₆₋₂₂ dimer. J Chem Theory Comput 15, 1440-1452.
- [38] Man VH, He X, Gao J, Wang J (2021) Effects of all-atom molecular mechanics force fields on amyloid peptide assembly: The case of the key hexapeptide PHF6 of tau protein. *J Chem Theory Comput* 17, 6458-6471.
- [39] Zoete V, Cuendet MA, Grosdidier A, Michielin O (2011) SwissParam, a fast force field generation tool for small organic molecules. J Comput Chem 32, 2359-2368.
- [40] Hess B, Kutzner C, van der Spoel D, Lindahl E (2008) Gromacs 4: Algorithms for highly efficient, load-balanced, and

- scalable molecular simulation. *J Chem Theory Comput* **4**, 435-447.
- [41] Berendsen HJC, Postma JPM, van Gunsteren WF, Dinola A, Haak JR (1984) Molecular dynamics with coupling to an external bath. J Chem Phys 81, 3684-3690.
- [42] Bussi G, Donadio D, Parrinello M (2007) Canonical sampling through velocity rescaling. J Chem Phys 126, 014101.
- [43] Hockney RW, Goel SP, Eastwood J (1974) Quit high resolution computer models of plasma. J Comp Phys 14, 148-158.
- [44] Hess B, Bekker H, Berendsen HJC, Fraaije JGEM (1997) LINCS: A linear constraint solver for molecular simulations. J Comp Chem 18, 1463-1472.
- [45] Darden T, York D, Pedersen L (1993) Particle mesh Ewald: An Nlog(N) method for Ewald sums in large systems. J Chem Phys 98, 10089-10092.
- [46] Frishman D, Argos P (1995) Knowledge-based secondary structure assignment. *Proteins* 23, 566-579.
- [47] Heinig M, Frishman D (2004) STRIDE: A Web server for secondary structure assignment from known atomic coordinates of proteins. *Nucleic Acids Res* 32, W500-W502.
- [48] Guo JL, Narasimhan S, Changolkar L, He Z, Stieber A, Zhang B, Gathagan RJ, Iba M, McBride JD, Trojanowski JQ, Lee VMY (2016) Unique pathological tau conformers from Alzheimer's brains transmit tau pathology in nontransgenic mice. J Exp Med 213, 2635-2654.
- [49] Nicoll JAR, Wilkinson D, Holmes C, Steart P, Markham H, Weller RO (2003) Neuropathology of human Alzheimer disease after immunization with amyloid-beta peptide: A case report. *Nat Med* 9, 448-452.
- [50] Hayden EY, Teplow DB (2013) Amyloid beta-protein oligomers and Alzheimer's disease. Alzheimers Res Ther 5, 60.
- [51] Limbocker R, Chia S, Ruggeri FS, Perni M, Cascella R, Heller GT, Meisl G, Mannini B, Habchi J, Michaels TCT, Challa PK, Ahn M, Casford ST, Fernando N, Xu CK, Kloss ND, Cohen SIA, Kumita JR, Cecchi C, Zasloff M, Linse S, Knowles TPJ, Chiti F, Vendruscolo M, Dobson CM (2019) Trodusquemine enhances Abeta(42) aggregation but suppresses its toxicity by displacing oligomers from cell membranes. Nat Commun 10, 225.
- [52] Shankar GM, Li S, Mehta TH, Garcia-Munoz A, Shepardson NE, Smith I, Brett FM, Farrell MA, Rowan MJ, Lemere CA, Regan CM, Walsh DM, Sabatini BL, Selkoe DJ (2008) Amyloid-R protein dimers isolated directly from Alzheimer's brains impair synaptic plasticity and memory. *Nat Med* 14, 837-842.
- [53] Ono K, Condron MM, Teplow DB (2009) Structureneurotoxicity relationships of amyloid β-protein oligomers. *Proc Natl Acad Sci U S A* 106, 14745-14750.
- [54] Mannini B, Mulvihill E, Sgromo C, Cascella R, Khodarahmi R, Ramazzotti M, Dobson CM, Cecchi C, Chiti F (2014) Toxicity of protein oligomers is rationalized by a function combining size and surface hydrophobicity. ACS Chem Biol 9, 2309-2317.
- [55] Sengupta U, Nilson AN, Kayed R (2016) The role of Amyloid-β oligomers in toxicity, propagation, and immunotherapy. EBioMedicine 6, 42-49.
- [56] Yang T, Li S, Xu H, Walsh DM, Selkoe DJ (2017) Large soluble oligomers of Amyloid β-protein from Alzheimer brain are far less neuroactive than the smaller oligomers to which they dissociate. *J Neurosci* 37, 152-163.
- [57] Jana MK, Cappai R, Pham CL, Ciccotosto GD (2016) Membrane-bound tetramer and trimer Aβ oligomeric

- species correlate with toxicity towards cultured neurons. *J Neurochem* **136**. 594-608.
- [58] Morgan C, Colombres M, Nunez MT, Inestrosa NC (2004) Structure and function of amyloid in Alzheimer's disease. *Prog Neurobiol* 74, 323-349.
- [59] Holmes BB, Furman JL, Mahan TE, Yamasaki TR, Mir-baha H, Eades WC, Belaygorod L, Cairns NJ, Holtzman DM, Diamond MI (2014) Proteopathic tau seeding predicts tauopathy in vivo. Proc Natl Acad Sci U S A 111, E4376-4385.
- [60] Bloom GS (2014) Amyloid-β and tau: The trigger and bullet in Alzheimer disease pathogenesis. JAMA Neurol 71, 505-508
- [61] Wischick CM, Edwards PC, Lai RYK, Rotht M, Harrington CR (1996) Selective inhibition of Alzheimer disease-like tau aggregation by phenothiazines. *Proc Natl Acad Sci U S A* 93, 11213-11218.
- [62] Taniguchi S, Suzuki N, Masuda M, Hisanaga S, Iwatsubo T, Goedert M, Hasegawa M (2005) Inhibition of heparin-induced tau filament formation by phenothiazines, polyphenols, and porphyrins. J Biol Chem 280, 7614-7623.
- [63] Ballatore C, Brunden KR, Piscitelli F, James MJ, Crowe A, Yao Y, Hyde E, Trojanowski JQ, Lee VM, Smith AB (2010) Discovery of brain-penetrant, orally bioavailable aminothienopyridazine inhibitors of tau aggregation. *J Med Chem* 53, 3739-3747.
- [64] Crowe A, James MJ, Lee VM, Smith AB, Trojanowski JQ, Ballatore C, Brunden KR (2013) Aminothienopyridazines and methylene blue affect tau fibrillization via cysteine oxidation. J Biol Chem 288, 11024-11037.
- [65] Fuse S, Matsumura K, Fujita Y, Sugimoto H, Takahash T (2014) Development of dual targeting inhibitors against aggregations of amyloid-β and tau protein. Eur J Med Chem 85, 228-234.
- [66] Lin CH, Hsieh YS, Wu YR, Hsu CJ, Chen HC, Huang WH, Chang KH, Hsieh-Li HM, Su MT, Sun YC, Lee GC, Lee-Chen GJ (2016) Identifying GSK-3β kinase inhibitors of Alzheimer's disease: Virtual screening, enzyme, and cell assays. Eur J Pharm Sci 89, 11-19.
- [67] Kondo K, Ikura T, Tanaka H, Fujita K, Takayama S, Yoshioka Y, Tagawa K, Homma H, Liu S, Kawasaki R, Huang Y, Ito N, ichi Tate S, Okazawa H (2021) HeptaHistidine inhibits Tau aggregation. ACS Chem Neurosci 12, 3015-3027.
- [68] Pujol-Pina R, Vilaprinylo-Pascual S, Mazzucato R, Arcella A, Vilaseca M, Orozco M, Carulla N (2015) SDS-PAGE analysis of Aβ oligomers is disserving research into Alzheimer's disease: Appealing for ESI-IM-MS. Sci Rep 5, 14809.
- [69] Viet MH, Ngo ST, Lam NS, Li MS (2011) Inhibition of aggregation of amyloid peptides by beta-sheet breaker peptides and their binding affinity. J Phys Chem B 115, 7433-7446.
- [70] Viet MH, Chen CY, Hu CK, Chen YR, Li MS (2013) Discovery of dihydrochalcone as a potential lead for Alzheimer's disease: *In silico* and *in vitro* study. *Plos One* 8, e79151.
- [71] Viet M. H, Gazova Z, Siposova K, Bednarikova Z, Antosova A, Trang NT, Li MS (2015) In silico and in vitro study of binding affinity of tripeptides to amyloid β fibrils: Implications for Alzheimer's disease. J Phys Chem B 119, 5145-5155.
- [72] Zwanzig RW (1954) High-temperature equation of state by a perturbation method. I. Nonpolar Gases. *J Chem Phys* 22, 1420.